

# Heterogeneous liquid-phase lactonization of 1,4-butanediol using $H_{3+x}PMo_{12-x}V_xO_{40}$ ( $x = 0-3$ ) catalysts immobilized on polyaniline

Seong Soo Lim<sup>a</sup>, Gyo Ik Park<sup>a</sup>, Jun Seon Choi<sup>a</sup>, In Kyu Song<sup>b</sup>, Wha Young Lee<sup>a,\*</sup>

<sup>a</sup> School of Chemical Engineering, Seoul National University, Shinlim-dong, Kwanak-ku, Seoul 151-742, South Korea

<sup>b</sup> Department of Industrial Chemistry, Kangnung National University, Kangnung, Kangwondo 210-702, South Korea

Received 28 September 2001; received in revised form 10 November 2001; accepted 30 November 2001

## Abstract

In order for successful application of heteropolyacids (HPAs) as heterogeneous catalysts to liquid-phase lactonization of 1,4-butanediol,  $H_{3+x}PMo_{12-x}V_xO_{40}$  ( $x = 0-3$ ) HPAs were immobilized on polyaniline (PANI) by one-step and two-step methods. Aniline was polymerized in the presence of HPA in the one-step preparation method, while HPA was immobilized on the ready-made PANI support in the two-step method. It was found that HPAs were molecularly dispersed and strongly immobilized in/on the PANI support as charge-compensating components. Most HPAs in the two-step HPA–PANI catalysts were immobilized only on the surface of PANI support. The surface areas of the two-step HPA–PANI catalysts were much higher than those of the one-step catalysts, which is important from the practical point of applications. Thermal stability of PANI support was much enhanced by the binding with HPA, and thermal stability of the two-step HPA–PANI catalysts was superior to the one-step catalysts. In the lactonization of 1,4-butanediol, catalytic activities were in the following order: two-step HPA–PANI > one-step HPA–PANI > unsupported HPA;  $H_6PMo_9V_3O_{40}$ –PANI >  $H_5PMo_{10}V_2O_{40}$ –PANI >  $H_4PMo_{11}V_1O_{40}$ –PANI >  $H_3PMo_{12}O_{40}$ –PANI. High activity of V-containing two-step catalysts and easiness of catalyst recovery in the liquid-phase reaction make them good candidates for an energy-saving lactonization process of 1,4-butanediol. © 2002 Elsevier Science B.V. All rights reserved.

**Keywords:** Heteropolyacid; Polyaniline; Immobilization; Heterogeneous liquid-phase reaction; Lactonization of 1,4-butanediol

## 1. Introduction

Heteropolyacids (HPAs) are inorganic acids as well as strong oxidizing agents [1–7]. Generally, the acid and redox catalytic properties of HPAs have been modified by replacing the protons with metal cations and/or by changing the heteroatom or the framework addenda atoms [8–11]. Other unique features that

make solid HPAs promising catalysts are their pseudo-liquid-phase behaviors and adsorption characteristics depending on the properties of adsorbates [12]. Vapor-phase oxidation of methacrolein into methacrylic acid [13–15] and hydration of isobutene into *tert*-butanol [16–18] are typical commercialized processes utilizing HPA as a heterogeneous catalyst and as a homogeneous catalyst, respectively.

Polymer materials have been widely used in chemical reactions as supports or catalysts [19–24]. Although application of polymer materials to chemical reactions at high temperatures has been restricted

\* Corresponding author. Tel.: +82-2-880-7404;

fax: +82-2-888-7295.

E-mail address: wyl@snu.ac.kr (W.Y. Lee).

due to their thermal and mechanical instability, much attention has also been paid to polymer materials because of their flexible applicability. As one of the promising approaches to the modification of novel catalysis of HPAs, polymer materials have also been introduced into the HPA catalyst system as supporting materials. One typical example can be found in the HPA–polymer composite film catalysts prepared by a membrane preparation technique, which takes advantage of solubility properties of HPA [25–28]. Another approach is to combine HPAs with ion-exchange resins such as poly-4-vinylpyridine [29] or conjugated conducting polymers such as polyaniline (PANI) and polypyrrole [30–38], by taking advantage of the overall negative charge of heteropolyanions. These HPA catalysts immobilized on conjugated conducting polymers have found successful applications as heterogeneous catalysts in some vapor-phase reactions such as ethanol and 2-propanol conversions. For example, it was reported that  $\text{H}_3\text{PMo}_{12}\text{O}_{40}$ –polyacetylene film catalyst exhibited higher activities for both oxidation and acid-catalytic reactions in the vapor-phase ethanol conversion than the bulk  $\text{H}_3\text{PMo}_{12}\text{O}_{40}$  [31]. On the other hand,  $\text{H}_3\text{PW}_{12}\text{O}_{40}$ –PANI [32] and  $\text{H}_3\text{PW}_{11}\text{Mo}_1\text{O}_{40}$ –PANI [36] catalysts were reported to show a higher oxidation activity but a lower acid-catalytic activity in the 2-propanol conversion than the corresponding solid bulk catalysts. Thus, conjugated conducting polymers have served as excellent supports for dispersion and immobilization of HPA catalysts, as far as heterogeneous vapor-phase oxidation reactions are concerned. The enhanced oxidation activities of HPA-conducting polymers have been understood in terms of any electronic modification of HPAs contributed by the characteristic reduction–oxidation property of conducting polymers [31,32,34], which distinguishes them from other types of polymer materials. That is also the reason why HPA-conducting polymer systems have been widely studied as electrode functionalization materials [35,39].

Two general preparation methods, one-step and two-step preparation, have been reported in the preparation of HPA-conducting polymer catalysts such as HPA–PANI [32]. In the one-step process, aniline is polymerized in the presence of HPA. Heteropolyanions are inevitably incorporated into the polymer matrix during the polymerization because the cationic

nature of the growing polymer chains requires the presence of anionic species to preserve the neutrality of the system. In the two-step preparation, aniline is polymerized in the absence of HPA, and then heteropolyanions are inserted into PANI via simple protonation reaction of ready-made polyemeraldine base. HPAs are anchored not only on the surface but also in the bulk of PANI support as a result of the one-step preparation. In the case of the two-step preparation, however, HPAs are immobilized only on the surface of PANI. It has been demonstrated that HPAs are bound with conjugated conducting polymers via quasi-ionic bond [32]. This means that the binding of HPA with conducting polymer is much stronger than any other interactions between HPAs and conventional inorganic supports. This makes HPA-conducting polymers good candidates as heterogeneous catalysts for liquid-phase reactions, as attempted in this work. The easiness of catalyst recovery in the heterogeneous liquid-phase reactions also allows us to expect an energy-saving catalytic process utilizing HPA-conducting polymer catalysts.

In this work,  $\text{H}_{3+x}\text{PMo}_{12-x}\text{V}_x\text{O}_{40}$  ( $x = 0–3$ ) catalysts were immobilized in/on PANI, and they were applied as heterogeneous catalysts to the liquid-phase lactonization of 1,4-butanediol into  $\gamma$ -butyrolactone. 1,4-Butanediol can be converted into a series of interesting chemicals via two major reactions, dehydration and dehydrogenation [40]. Dehydration produces tetrahydrofuran (THF), which is useful as a solvent and as a precursor for polytetramethylene ether glycol (PTMEG). Dehydrogenation of 1,4-butanediol leads to  $\gamma$ -butyrolactone, which is an important chemical as a solvent and as a precursor for *N*-methyl-2-pyrrolidone and 2-pyrrolidone. It is known that HPA catalysts are active in the lactonization of 1,4-butanediol [41–43].

## 2. Experimental

### 2.1. Preparation of HPA–PANI catalysts

$\text{H}_3\text{PMo}_{12}\text{O}_{40}$  ( $\text{PMo}_{12}$ ) catalysts immobilized on PANI were prepared by one-step and two-step procedures, according to published methods [32–38]. Solid  $\text{PMo}_{12}$  catalyst and organic chemicals used in this work were purchased from Aldrich Chemical Co.  $\text{PMo}_{12}$  catalyst was thermally treated at 300 °C for

the precise quantification prior to use. In the one-step preparation of  $\text{PMo}_{12}$ -PANI, 3.9 ml of distilled aniline and 16.8 g of  $\text{PMo}_{12}$  were dissolved in 250 ml of  $\text{CH}_3\text{CN}$  (ACN). An amount of 7.85 g of  $(\text{NH}_4)_2\text{S}_2\text{O}_8$  was dissolved in 9 ml of water, and then this solution was added dropwise into the  $\text{PMo}_{12}$ -aniline-ACN solution. After 24 h polymerization at room temperature, the reaction was terminated by precipitation of the solid product in excess amounts of methanol. The solid product was washed several times successively with methanol, diethylether, and water until the washing solvents became colorless, and then it was dried to yield the final form. The resultant catalyst was abbreviated as  $\text{PMo}_{12}$ -PANI(I) by the sequence of catalyst-PANI (preparation step).

For the two-step preparation of  $\text{PMo}_{12}$ -PANI catalysts, the emeraldine salt (PANIS) of PANI was purchased from Aldrich Chemical Co. Deprotonation of PANIS was achieved in 3% aqueous  $\text{NH}_4\text{OH}$  solution to obtain emeraldine base (PANIB), according to the method in [32]. Immobilization of  $\text{PMo}_{12}$  on the surface of PANIB was done by the reaction (protonation) of PANIB (5 g) with  $\text{PMo}_{12}$  (1 g) dissolved in ACN (200 ml). The solid product was washed and dried as described above. The resultant catalyst was abbreviated as  $\text{PMo}_{12}$ -PANI(II) by the sequence of catalyst-PANI (preparation step).

Vanadium-containing mixed addenda HPAs,  $\text{H}_{3+x}\text{PMo}_{12-x}\text{V}_x\text{O}_{40}$  ( $x = 1-3$ ), were also immobilized on PANI supports. These mother HPAs were purchased from Nippon Inorganic Color and Chemical Co. As described above,  $\text{H}_{3+x}\text{PMo}_{12-x}\text{V}_x\text{O}_{40}$  ( $x = 1-3$ )-PANI catalysts were prepared by one-step and two-step methods. In the one-step preparation, 50 ml of aniline, 3 g of HPA, 400 ml of ACN, and 20 g of  $(\text{NH}_4)_2\text{S}_2\text{O}_8$  were used. The polymerization was carried out at 15 °C for 24 h. In the two-step preparation, 5 g of PANIB, 0.5 g of HPA, and 200 ml of ACN were used. Abbreviation of the resulting catalysts was the same as  $\text{PMo}_{12}$ -PANI catalyst systems. For example,  $\text{PMo}_{11}\text{V}_1$ -PANI(II) represents  $\text{H}_4\text{PMo}_{11}\text{V}_1\text{O}_{40}$  catalyst immobilized on PANIB via two-step preparation method.

## 2.2. Reaction and characterization

Heterogeneous liquid-phase lactonization of 1,4-butanediol was carried out in a constantly stirred

batch-wise Pyrex reactor with a reflux condenser. An amount of 30 ml of *tert*-butanol (reaction medium) and 0.2 g of HPA-PANI catalyst were charged into the stirred reactor under  $\text{N}_2$  stream. Then the reactor was heated up and maintained at 80 °C for 30 min. The reaction was initiated by introducing 1,4-butanediol (5 ml) and  $\text{H}_2\text{O}_2$  (34%, 2 ml) into the reactor by a syringe. Vaporized *tert*-butanol was condensed and refluxed to the reactor continuously. After 20 h reaction in each run, the product was sampled and analyzed with a GC equipped with an FID.

In order to confirm the HPA immobilization on the PANI supports, FT-IR studies of the unsupported and immobilized catalysts were carried out on a BOMEM MB-100 spectrometer equipped with a NaCl window using a KBr pressed-pellet technique. All the samples were previously evacuated at 100 °C for 30 min for the FT-IR measurements. Thermal stabilities of the supports and immobilized catalysts were examined by performing thermogravimetry analyses (TGAs) on a Perkin-Elmer TGA7 instrument. In the measurements, identical amount of sample (6 mg) was used for each run, and thermal scanning was done at temperatures ranging from 100 to 600 °C at the heating rate of 10 °C/min with an air flow (20 ml/min). XRD patterns of the catalysts were obtained using a Rigaku MXP-18XHF32 diffractometer with  $\text{Cu K}\alpha$  radiation at the scanning rate of 5°/min. Surface areas of the samples were measured by BET method on a Micromeritics ASAP2010 analyzer using nitrogen as an adsorbed gas. Elemental analyses of the supported catalysts were done by ICP method using a VG PQ-2 TURBO instrument.

## 3. Results and discussion

### 3.1. Immobilization of $\text{PMo}_{12}$ on PANI support

Immobilization of  $\text{PMo}_{12}$  on PANI in the  $\text{PMo}_{12}$ -PANI catalysts was confirmed by FT-IR analyses, as shown in Fig. 1. The primary structure, the Keggin structure [44], of  $\text{PMo}_{12}\text{O}_{40}^{3-}$  can be identified by the observation of four characteristic IR bands ranging from 700 to 1100  $\text{cm}^{-1}$  [2,45]. Four IR bands of the unsupported  $\text{PMo}_{12}$  catalyst were observed at 1064 (P-O band), 964 (Mo=O band), 868 and 789  $\text{cm}^{-1}$  (Mo-O-Mo bands). IR spectrum of PANIB was

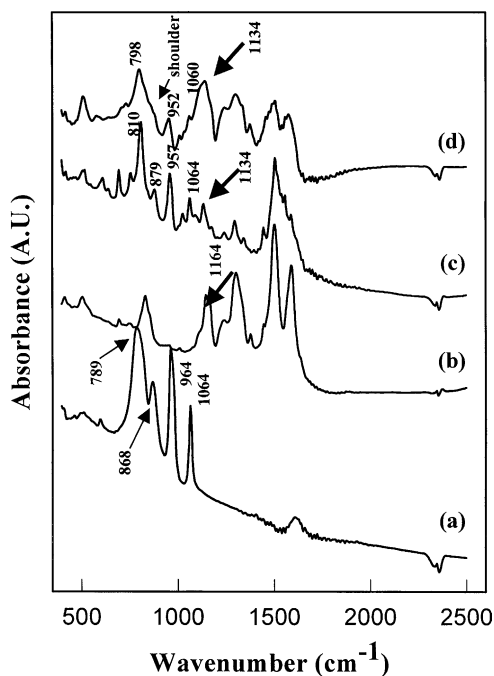


Fig. 1. IR spectra of (a) unsupported  $\text{PMO}_{12}$ , (b) PANIB, (c)  $\text{PMO}_{12}$ -PANI(I) and (d)  $\text{PMO}_{12}$ -PANI(II) samples.

basically different from that of either  $\text{PMO}_{12}$ -PANI(I) or  $\text{PMO}_{12}$ -PANI(II) sample. The four characteristic IR bands of  $\text{PMO}_{12}$  in  $\text{PMO}_{12}$ -PANI(I) and  $\text{PMO}_{12}$ -PANI(II) catalysts were observed at slightly shifted positions, compared to those of the unsupported  $\text{PMO}_{12}$ . In fact, these shifts might be due to some reasons; overlapping of spectra of  $\text{PMO}_{12}$  and PANI, any unexpected interaction between  $\text{PMO}_{12}$  and KBr matrix, or genuine interaction between  $\text{PMO}_{12}$  and PANI formed via immobilization. More importantly, however, a strong IR band at  $1164\text{ cm}^{-1}$  observed in PANIB sample, the characteristic band of the non-protonated base form, became weak in both  $\text{PMO}_{12}$ -PANI(I) and  $\text{PMO}_{12}$ -PANI(II) catalysts. Furthermore, an IR band at  $1134\text{ cm}^{-1}$ , the characteristic band of the protonated states, clearly appeared in both  $\text{PMO}_{12}$ -PANI catalysts, as demonstrated in a previous report [32]. These results clearly show that  $\text{PMO}_{12}$  was successfully immobilized on the PANI matrix in both catalysts as a charge-compensating component.

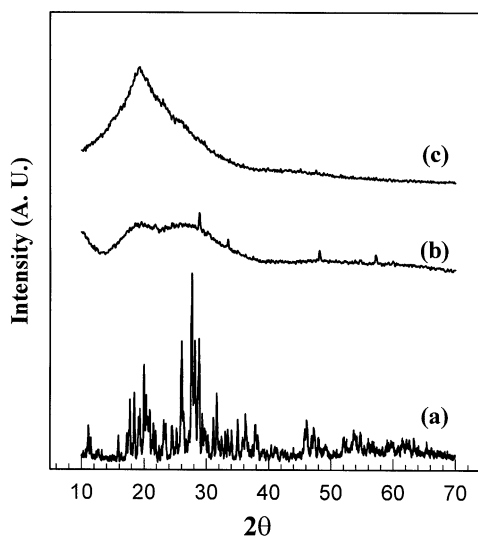


Fig. 2. XRD patterns of (a) unsupported  $\text{PMO}_{12}$ , (b)  $\text{PMO}_{12}$ -PANI(I) and (c)  $\text{PMO}_{12}$ -PANI(II) catalysts.

### 3.2. Dispersion of $\text{PMO}_{12}$ on PANI support

Fig. 2 shows the XRD patterns of unsupported  $\text{PMO}_{12}$  and  $\text{PMO}_{12}$ -PANI catalysts. PANIB showed no characteristic XRD patterns due to its amorphous nature. It is noticeable that  $\text{PMO}_{12}$ -PANI(II) catalyst also showed no characteristic XRD patterns. This result represents that  $\text{PMO}_{12}$  catalyst in the  $\text{PMO}_{12}$ -PANI(II) did not exist as a crystalline form, but instead was highly dispersed as fine particles on the PANI matrix. It is believed that  $\text{PMO}_{12}$  was selectively immobilized on the cationic sites of PANI matrix in the  $\text{PMO}_{12}$ -PANI(II) catalyst via quasi-ionic bond [32], and consequently,  $\text{PMO}_{12}$  would be finely dispersed in the support. On the other hand,  $\text{PMO}_{12}$ -PANI(I) catalyst showed weak XRD peaks, which are different in positions and intensities from those of the unsupported  $\text{PMO}_{12}$ . Upon reducing the portion of  $\text{PMO}_{12}$  in the preparation of  $\text{PMO}_{12}$ -PANI(I) catalyst, however, the resulting catalyst exhibited an amorphous XRD pattern with no peak-like features. Considering that XRD pattern of an HPA reflects its secondary structure which strongly depends on its environments even in a single HPA compound [2], it is inferred that the weak XRD peaks observed for  $\text{PMO}_{12}$ -PANI(I) catalyst were possibly due to unsuccessfully immobilized  $\text{PMO}_{12}$  clusters (just trapped in the PANI) in

Table 1  
Empirical formulas and surface areas of PMO<sub>12</sub>–PANI catalysts

Catalyst	Empirical formula determined by ICP	Weight content of PMO <sub>12</sub> (wt.%)	BET surface area (m <sup>2</sup> /g)
PMO <sub>12</sub> –PANI(I)	C <sub>6</sub> H <sub>4.5</sub> N(PMO <sub>12</sub> ) <sub>0.0831</sub>	62.6	49.4
PMO <sub>12</sub> –PANI(II)	C <sub>6</sub> H <sub>4.5</sub> N(PMO <sub>12</sub> ) <sub>0.0214</sub>	23.3	139.9

the one-step polymerization process. It can also be inferred that the environments of these PMO<sub>12</sub> components would be different from those of the unsupported catalyst, which produced non-identical XRD patterns as observed in Fig. 2(a) and (b). Although all the PMO<sub>12</sub> ingredients in the PMO<sub>12</sub>–PANI(I) catalyst were not finely dispersed enough to show an amorphous XRD behavior, it is believed that the PMO<sub>12</sub>–PANI(I) catalyst may have comparable surface dispersion of PMO<sub>12</sub> to the PMO<sub>12</sub>–PANI(II) catalyst.

### 3.3. Surface area and elemental analysis

Empirical formulas and surface areas of PMO<sub>12</sub>–PANI catalysts determined by ICP and BET measurements, respectively, are summarized in Table 1. The amount of PMO<sub>12</sub> in the one-step PMO<sub>12</sub>–PANI(I) was much larger than that in the two-step PMO<sub>12</sub>–PANI(II) catalyst, as previously demonstrated in [32]. In a previous work [37], it was also reported that the maximum HPA content with respect to aniline monomer in the two-step HPA–PANI catalysts could not exceed 0.03, which is in good agreement with the result observed for PMO<sub>12</sub>–PANI(II) catalyst. BET surface area of PMO<sub>12</sub>–PANI(II) was much higher than that of PMO<sub>12</sub>–PANI(I), in a general fashion that surface area is inversely proportional to the PMO<sub>12</sub> content. All these results support that PMO<sub>12</sub> was anchored not only on the surface but also in the bulk of PMO<sub>12</sub>–PANI(I) catalyst, whereas PMO<sub>12</sub> was mainly immobilized on the surface of PMO<sub>12</sub>–PANI(II) catalyst, which is of great importance from the practical point of view of catalytic applications.

### 3.4. Thermal stability of PMO<sub>12</sub>–PANI catalysts

Fig. 3 shows the thermogravimetries of PANI and PMO<sub>12</sub>–PANI samples. Thermal scanning was done at temperatures ranging from 100 to 600 °C over the identical amount of sample for each run. Scanning

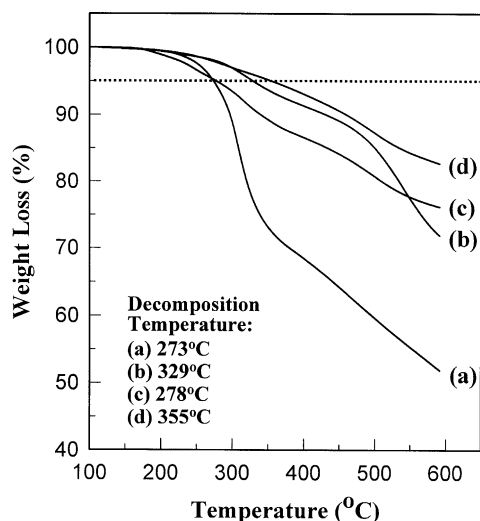


Fig. 3. Thermogravimetry analyses of (a) PANIS, (b) PANIB, (c) PMO<sub>12</sub>–PANI(I) and (d) PMO<sub>12</sub>–PANI(II) samples; heating rate = 10 °C/min.

at temperatures below 100 °C was not done because slight weight changes in this region were not associated with the decomposition of PANI but with the release of solvents and water from the samples. According to the conventional definition generally used in polymer sciences, the temperature at which 5% loss of the initial weight was detected was taken as the decomposition temperature of the polymer. The decomposition temperatures of PANI and PMO<sub>12</sub>–PANI samples were also presented in Fig. 3. These decomposition temperatures are below the thermal decomposition temperature of PMO<sub>12</sub> catalyst, which is known to be near 400 °C [46,47]. This means that the decomposition temperatures are attributed to only PANI ingredient in the samples. Fig. 3 also shows that thermal stability of PANIB was superior to PANIS, and furthermore, thermal stability of two-step PMO<sub>12</sub>–PANI(II) catalyst was much superior to one-step PMO<sub>12</sub>–PANI(I) catalyst.

Table 2  
Empirical formulas and surface areas of  $\text{PMo}_{12-x}\text{V}_x$  ( $x = 1-3$ )-PANI catalysts

Catalyst	Empirical formula determined by ICP	Weight content of $\text{PMo}_{12-x}\text{V}_x$ (wt.%)	BET surface area ( $\text{m}^2/\text{g}$ )
$\text{PMo}_{11}\text{V}_1$ -PANI(I)	$\text{C}_6\text{H}_{4.5}\text{N}(\text{PMo}_{11}\text{V}_1)_{0.0435}$	47.4	70.1
$\text{PMo}_{11}\text{V}_1$ -PANI(II)	$\text{C}_6\text{H}_{4.5}\text{N}(\text{PMo}_{11}\text{V}_1)_{0.0067}$	11.4	183.9
$\text{PMo}_{10}\text{V}_2$ -PANI(I)	$\text{C}_6\text{H}_{4.5}\text{N}(\text{PMo}_{10}\text{V}_2)_{0.0489}$	48.3	51.8
$\text{PMo}_{10}\text{V}_2$ -PANI(II)	$\text{C}_6\text{H}_{4.5}\text{N}(\text{PMo}_{10}\text{V}_2)_{0.0090}$	14.7	100.3
$\text{PMo}_9\text{V}_3$ -PANI(I)	$\text{C}_6\text{H}_{4.5}\text{N}(\text{PMo}_9\text{V}_3)_{0.0436}$	44.8	65.8
$\text{PMo}_9\text{V}_3$ -PANI(II)	$\text{C}_6\text{H}_{4.5}\text{N}(\text{PMo}_9\text{V}_3)_{0.0084}$	13.6	142.1

Importantly,  $\text{PMo}_{12}$ -PANI(II) was more thermally stable than the mother support (PANIB), representing that thermal stability of PANIB was much enhanced by the binding with  $\text{PMo}_{12}$ . This result also means that  $\text{PMo}_{12}$  did not serve as a mere additive for PANI, and that the interaction between  $\text{PMo}_{12}$  and PANI support was not physical.

### 3.5. Characteristics of $\text{PMo}_{12-x}\text{V}_x$ ( $x = 1-3$ )-PANI catalysts

$\text{PMo}_{12-x}\text{V}_x$  ( $x = 1-3$ )-PANI catalysts were also prepared by one-step and two-step methods as described earlier. Empirical formulas and surface areas of  $\text{PMo}_{12-x}\text{V}_x$ -PANI catalysts determined by ICP and BET measurements, respectively, are summarized in Table 2. As previously observed for the  $\text{PMo}_{12}$ -PANI catalysts, the amounts of  $\text{PMo}_{12-x}\text{V}_x$  in the two-step  $\text{PMo}_{12-x}\text{V}_x$ -PANI(II) catalysts were much smaller than those in the one-step  $\text{PMo}_{12-x}\text{V}_x$ -PANI(I) catalysts. The HPA weight contents were in the range of 44–49% for the  $\text{PMo}_{12-x}\text{V}_x$ -PANI(I) catalysts, and 11–19% for the  $\text{PMo}_{12-x}\text{V}_x$ -PANI(II) catalysts. The HPA contents with respect to aniline monomer in the  $\text{PMo}_{12-x}\text{V}_x$ -PANI(II) catalysts were found not to exceed 0.03. As expected, BET surface areas of the  $\text{PMo}_{12-x}\text{V}_x$ -PANI(II) catalysts were much higher than those of the corresponding  $\text{PMo}_{12-x}\text{V}_x$ -PANI(I) catalysts, in the same fashion as those observed for the  $\text{PMo}_{12}$ -PANI catalysts. All these results suggest that  $\text{PMo}_{12-x}\text{V}_x$  ingredients in the two-step  $\text{PMo}_{12-x}\text{V}_x$ -PANI(II) catalysts were mainly immobilized only on the surface.

Dispersion of  $\text{PMo}_{12-x}\text{V}_x$  ( $x = 1-3$ ) catalyst in/on PANI support was precisely examined by XRD analyses. A typical example is shown in Fig. 4 for

the case of  $\text{PMo}_9\text{V}_3$ -based catalysts. The intensity of the diffracted radiation was plotted as a function of wave vector  $q$  defined as  $4\pi \sin\theta/\lambda$ , where  $\theta$  and  $\lambda$  represent X-ray diffraction angle and wavelength, respectively. As can be seen from the deconvoluted curves for each sample, the peak originating from PANI chain at  $q \approx 1.3 \text{ \AA}^{-1}$  (Fig. 4(a)) became broad and split into two peaks upon  $\text{PMo}_9\text{V}_3$  immobilization. This indicates that PANI chain was somewhat disordered and experienced structural changes upon  $\text{PMo}_9\text{V}_3$  immobilization. As also shown in Fig. 4,  $\text{PMo}_9\text{V}_3$ -PANI(I) sample exhibited a well-developed sharp peak at  $q \approx 0.51 \text{ \AA}^{-1}$  ( $d$ -spacing  $\approx 12.4 \text{ \AA}$ ), while  $\text{PMo}_9\text{V}_3$ -PANI(II) sample showed an intensity curve under developing in the region smaller than  $q \approx 0.51 \text{ \AA}^{-1}$ . Although the maximum point was not detected in the  $\text{PMo}_9\text{V}_3$ -PANI(II) sample in that region, the intensity maximum would be at a smaller  $q$ -value than the lower bound of  $q$  ( $\approx 0.31 \text{ \AA}^{-1}$ ) which corresponds to the  $d$ -spacing of  $20.2 \text{ \AA}$ . When taking into account the size of the Keggin-type [44] HPA (ca.  $10-12 \text{ \AA}$ ), these results suggest that  $\text{PMo}_9\text{V}_3$  was molecularly dispersed in both  $\text{PMo}_9\text{V}_3$ -PANI(I) and  $\text{PMo}_9\text{V}_3$ -PANI(II).

### 3.6. Lactonization of 1,4-butanediol by $\text{PMo}_{12-x}\text{V}_x$ ( $x = 0-3$ )-PANI catalysts

Fig. 5 shows the catalytic activities of  $\text{PMo}_{12-x}\text{V}_x$  ( $x = 0-3$ )-PANI catalysts in the liquid-phase lactonization of 1,4-butanediol into  $\gamma$ -butyrolactone. The reaction was carried out for 20 h in each run to yield considerable amounts of product for comparison. Catalytic activities with respect to the preparation method were in the following order:  $\text{PMo}_{12-x}\text{V}_x$  ( $x = 0-3$ )-PANI(II) >  $\text{PMo}_{12-x}\text{V}_x$

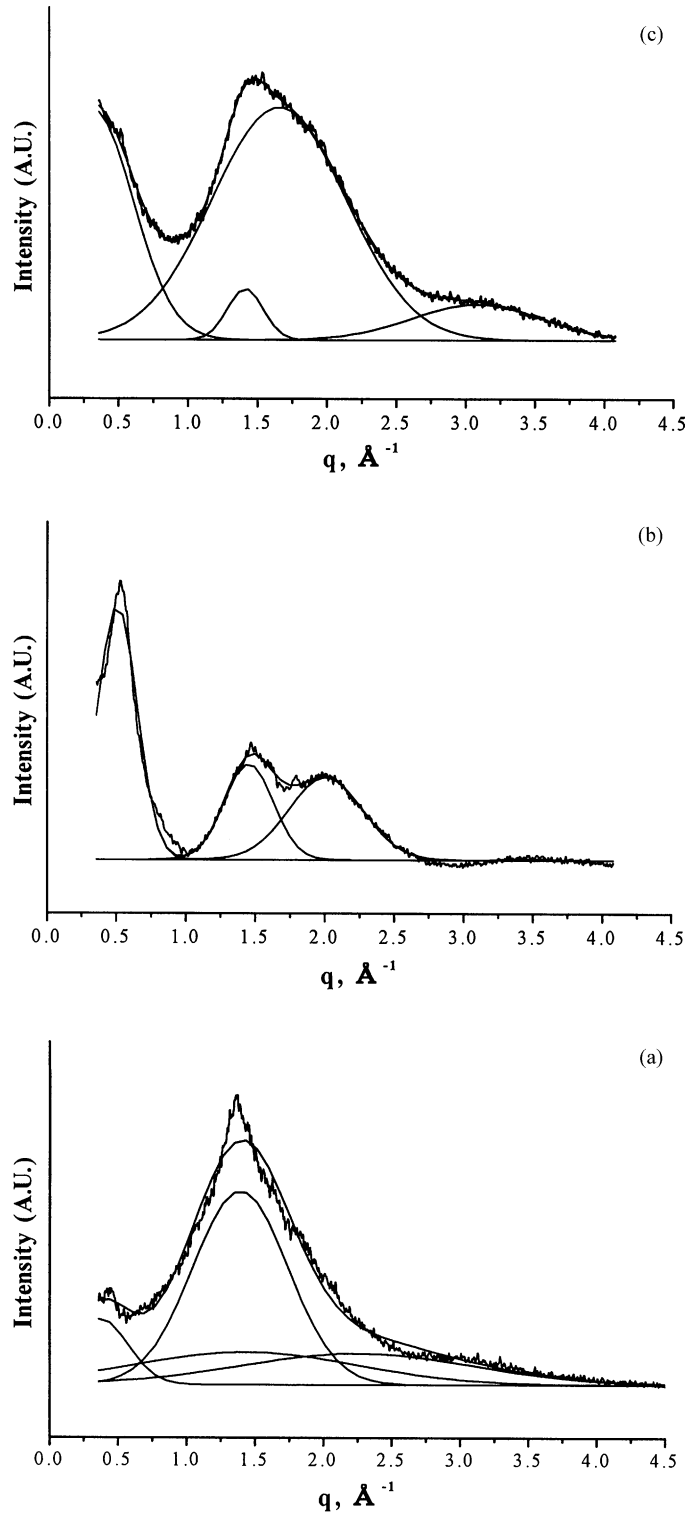


Fig. 4. XRD analyses of (a) PANIB, (b)  $\text{PMo}_9\text{V}_3\text{-PANI(I)}$  and (c)  $\text{PMo}_9\text{V}_3\text{-PANI(II)}$ .

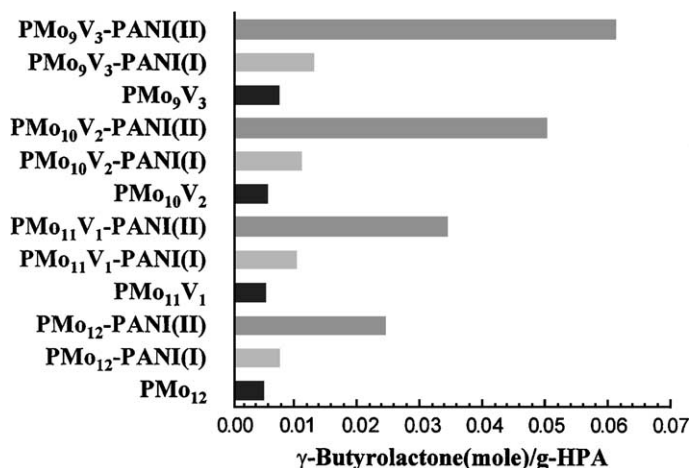


Fig. 5. Productivity of  $\gamma$ -butyrolactone from 1,4-butanediol by unsupported PMo<sub>12-x</sub>V<sub>x</sub> ( $x = 0-3$ ) and PMo<sub>12-x</sub>V<sub>x</sub> ( $x = 0-3$ )-PANI catalysts in the liquid-phase reaction; reaction temperature = 80 °C, reaction time = 20 h, catalyst = 0.2 g, *tert*-butanol = 30 ml, 1,4-butanediol = 5 ml, H<sub>2</sub>O<sub>2</sub> (34%) = 2 ml.

( $x = 0-3$ )-PANI(I) > unsupported PMo<sub>12-x</sub>V<sub>x</sub> ( $x = 0-3$ ). The enhanced activities of the one-step and two-step catalysts compared to the corresponding unsupported catalysts were attributed to the following two factors: one is the molecular-level dispersion of PMo<sub>12-x</sub>V<sub>x</sub> ( $x = 0-3$ ) catalyst in/on PANI support, and the other might be a certain electronic modification of PMo<sub>12-x</sub>V<sub>x</sub> ( $x = 0-3$ ) catalyst contributed by PANI support via ionic immobilization, as demonstrated in some gas–solid reactions over the HPA-conjugated conducting polymer catalysts [31,32,34]. The enhanced activities of the two-step PMo<sub>12-x</sub>V<sub>x</sub> ( $x = 0-3$ )-PANI(II) catalysts compared to the corresponding one-step catalysts were believed to be due to the fact that PMo<sub>12-x</sub>V<sub>x</sub> ( $x = 0-3$ ) HPAs were mainly immobilized on the surface of the two-step catalysts; the two-step catalysts yield high surface areas and efficiently provide surface species active for the reaction. The catalytic activities with respect to the HPA identity were in the following order: PMo<sub>9</sub>V<sub>3</sub>-PANI > PMo<sub>10</sub>V<sub>2</sub>-PANI > PMo<sub>11</sub>V<sub>1</sub>-PANI > PMo<sub>12</sub>-PANI. Thus, high catalytic performance of V-containing two-step catalysts and easiness of catalyst recovery in the liquid-phase reaction make them good candidates suitable for an energy-saving lactonization process of 1,4-butanediol.

#### 4. Conclusions

In this work, PMo<sub>12-x</sub>V<sub>x</sub> ( $x = 0-3$ )-PANI catalysts were prepared by one-step and two-step methods, and they were used as heterogeneous catalysts in the liquid-phase lactonization of 1,4-butanediol. HPA catalysts were molecularly dispersed and strongly immobilized in/on the PANI support as charge-compensating components. Most HPA ingredients in the two-step HPA–PANI catalysts were immobilized only on the surface of PANI matrix, and therefore, the surface areas of the two-step HPA–PANI were much higher than those of the one-step catalysts. Thermal stability of PANI support was much enhanced by the binding with HPA, and thermal stability of the two-step HPA–PANI catalysts was superior to the one-step catalysts. In the heterogeneous lactonization of 1,4-butanediol, HPA–PANI catalysts showed higher performances than the unsupported mother catalysts, and HPA–PANI catalysts prepared by two-step method showed better performances than those prepared by one-step method. The catalytic activities with respect to the HPA identity were in the following order: PMo<sub>9</sub>V<sub>3</sub>-PANI > PMo<sub>10</sub>V<sub>2</sub>-PANI > PMo<sub>11</sub>V<sub>1</sub>-PANI > PMo<sub>12</sub>-PANI. The easiness of catalyst recovery in the liquid-phase reaction also makes vanadium-containing two-step catalysts good



candidates for an energy-saving lactonization process of 1,4-butanediol.

## Acknowledgements

The authors acknowledge the research fund from LG Chem. Ltd. for this work.

## References

- [1] M. Misono, *Mater. Chem. Phys.* 17 (1987) 103.
- [2] T. Okuhara, N. Mizuno, M. Misono, *Adv. Catal.* 41 (1996) 113.
- [3] H. Hayashi, J.B. Moffat, *J. Catal.* 81 (1983) 66.
- [4] N. Mizuno, M. Misono, *Chem. Rev.* 98 (1998) 199.
- [5] C.L. Hill, C.M. Prosser-McCartha, *Coord. Chem. Rev.* 143 (1995) 407.
- [6] I.V. Kozhevnikov, *Catal. Rev.-Sci. Eng.* 37 (1995) 311.
- [7] T. Yokota, S. Fujibayashi, Y. Nishiyama, S. Sakaguchi, Y. Ishii, *J. Mol. Catal. A* 114 (1996) 113.
- [8] K. Urabe, K. Fujita, Y. Izumi, *Shokubai* 22 (1980) 223.
- [9] T. Okuhara, T. Nishimura, K. Ohashi, M. Misono, *Chem. Lett.* (1990) 1201.
- [10] H.C. Kim, S.H. Moon, W.Y. Lee, *Chem. Lett.* (1991) 447.
- [11] G.B. McGarvey, J.B. Moffat, *J. Catal.* 128 (1991) 69.
- [12] M. Misono, K. Sakata, Y. Yoneda, W.Y. Lee, *Stud. Surf. Sci. Catal.* 7B (1980) 1047.
- [13] N. Mizuno, T. Watanabe, M. Misono, *Bull. Chem. Soc. Jpn.* 64 (1991) 243.
- [14] H. Mori, N. Mizuno, M. Misono, *J. Catal.* 131 (1990) 133.
- [15] M. Ai, *J. Catal.* 71 (1981) 88.
- [16] M. Misono, *Catal. Rev.-Sci. Eng.* 29 (1987) 269.
- [17] A. Aoshima, S. Yamamatsu, T. Yamaguchi, *Nippon Kagaku Kaishi* (1987) 1768.
- [18] A. Aoshima, S. Yamamatsu, T. Yamaguchi, *Nippon Kagaku Kaishi* (1987) 1763.
- [19] V.P. Gupta, W.J.M. Douglas, *AIChE J.* 13 (1967) 883.
- [20] S.K. Ihm, M.J. Chung, K.Y. Park, *Ind. Eng. Chem. Res.* 27 (1988) 41.
- [21] C. Iditoiu, E. Segal, B.C. Gates, *J. Catal.* 54 (1978) 442.
- [22] K.M. Dooley, J.A. Williams, B.C. Gates, R.L. Albright, *J. Catal.* 74 (1982) 361.
- [23] E. Ruckenstein, L. Hong, *J. Catal.* 136 (1992) 378.
- [24] L. Hong, E. Ruckenstein, *Reactive Polym.* 16 (1992) 181.
- [25] J.K. Lee, I.K. Song, W.Y. Lee, *J. Mol. Catal. A* 120 (1997) 207.
- [26] S.S. Lim, Y.H. Kim, G.I. Park, W.Y. Lee, I.K. Song, H.K. Youn, *Catal. Lett.* 60 (1999) 199.
- [27] G.I. Park, S.S. Lim, J.S. Choi, I.K. Song, W.Y. Lee, *J. Catal.* 178 (1998) 378.
- [28] W.Y. Lee, I.K. Song, J.K. Lee, G.I. Park, S.S. Lim, *Korean J. Chem. Eng.* 14 (1997) 432.
- [29] K. Nomiya, H. Murasaki, M. Miwa, *Polyhedron* 5 (1986) 1031.
- [30] A. Proń, *Synth. Met.* 46 (1992) 227.
- [31] J. Poźniczek, I. Kulszewicz-Bajer, M. Zagórska, K. Kruczała, K. Dyrek, A. Bielański, A. Proń, *J. Catal.* 132 (1991) 311.
- [32] M. Hasik, W. Turek, E. Stochmal, M. Łapkowski, A. Proń, *J. Catal.* 147 (1994) 544.
- [33] J. Poźniczek, A. Bielański, I. Kulszewicz-Bajer, M. Zagórska, K. Kruczała, K. Dyrek, A. Proń, *J. Mol. Catal.* 69 (1991) 223.
- [34] R. Dziembaj, A. Małecka, Z. Piwowska, A. Bielański, *J. Mol. Catal. A* 112 (1996) 423.
- [35] S. Dong, W. Jin, *J. Electroanal. Chem.* 354 (1993) 87.
- [36] L.-Y. Qu, R.-Q. Lu, J. Peng, Y.-G. Chen, Z.-M. Dai, *Synth. Met.* 84 (1997) 135.
- [37] M. Hasik, A. Proń, *New J. Chem.* 19 (1995) 1155.
- [38] K. Pielichowski, M. Hasik, *Synth. Met.* 89 (1997) 199.
- [39] A. Yamada, J.B. Goodenough, *J. Electrochem. Soc.* 145 (1998) 737.
- [40] M. Morgan, *Chem. Ind.* (1997) 166.
- [41] Y. Ishii, T. Yoshida, K. Yamawaki, M. Ogawa, *J. Org. Chem.* 53 (1988) 5549.
- [42] Y. Ishii, K. Yamawaki, T. Yoshida, T. Ura, M. Ogawa, *J. Org. Chem.* 52 (1987) 1868.
- [43] B. Török, I. Busci, T. Beregszászi, I. Kapocsi, Á. Molnár, *J. Mol. Catal. A* 107 (1996) 305.
- [44] J.F. Keggin, *Nature* 131 (1933) 908.
- [45] C. Rocchiccioli-Deltcheff, R. Thouvenot, R. Franck, *Spectrochim. Acta A* 32 (1976) 587.
- [46] M. Fournier, C.F. Jantos, C. Rabia, G. Herve, S. Launay, *J. Mater. Chem.* 2 (1992) 971.
- [47] C. Rocchiccioli-Deltcheff, A. Aouissi, M.M. Bettahar, S. Launay, M. Fournier, *J. Catal.* 164 (1996) 16.